Research Article: Open Access

VIBGYOR ePress

International Journal of Optics and Photonic Engineering

ISSN: 2631-5092

Optical Properties of Non-Malignant and Malignant Breast Tissue Determined by Surface Displacement of Laser-Induced Photoacoustic Generation

Yasser H El-Sharkawy*

Department of Biomedical Engineering, Military Technical College, Egypt

Abstract

Purpose: Time-resolved photoacoustic response has been used to characterize breast tissues for the purpose of discriminating between normal and cancerous tumor areas of tissue. The physical response of biological tissue to a short laser pulse is primary thermo mechanical.

Methods: In this work, ultrasonic thermo elastic waves were generated in breast tissue by the absorption of nanosecond laser pulses at 1064 nm produced by a Q-switched Nd: YAG laser in conjunction with an optical interferometer sensor was used to detect the thermo elastic deformation.

Results: At 1064 nm, differences in photoacoustic response signatures of non-malignant and malignant human breast tissue were found to be highly enhanced.

Conclusion: This study yields information about the laser-tissue interaction and determines properties of breast tissue samples could be used as diagnostic parameters.

Keywords

Photo acoustic response, Characterizing breast tissue, Optical sensor

Introduction

It has been estimated that one out of every nine women will develop breast cancer during her lifetime and approximately 30% of them will die of the disease [1,2].

The beneficial effect of screening mammography has been shown in several studies world-wide where 20%-50% reduction in breast cancer mortality with screening has been demonstrated [3-9]. In general, the smaller the lesion at the time of detection, the better the treatment efficiency [10,11]. Conversely, while mammography has clearly become the method of choice in the detection of early, clinically occult breast cancer, it has limitations. First, of all the breast cancers, only averages of 88% are seen on mammography [12]. Secondly the positive predictive value PPV for mammographic screening ranges from 3% to 38%. The variability of PPV values reported in the literature depends on the patient age, on issues pertaining to how the study was performed and on the systematic screening follow-up of selected low suspicious lesions [13,14]. For an estimated 150,000new cases of breast cancer diagnosed employing biopsy each year and an average of 20% true positive rate, approximately 750,000 breast biopsies will be performed to make these diagnoses. The lack of mammographic specificity subjects many women with benign breast disease to unnecessary biopsy. In fact, it has been estimated that the expense of biopsies is the major cost of screening mammography programs, accounting for 32.2%, slightly more than the cost of the mammograms themselves [15].

In the last decade, photoacoustic imaging has emerged as a potent imaging method enabling to non-invasively study processes and structures at the interior of biological samples such as small animals. The method synergistically combines the advantages of optical imaging, i.e., high optical contrast with the advantages of acoustical imaging (sonography), i.e., high resolutions at large penetration depths [16].

In consequence, it did not take much time until photoacoustic imaging of tumors found attention, setting the base for biological investigations that had afore been reserved for radiological, ionizing or invasive imaging methods [17]. Also around the turn of the millennium, reconstruction algorithms for performing photoacoustic tomography were presented. Among all biomedical imaging modalities that are applicable for preclinical mesoscopy, like X-Ray computed tomography (XCT) or magnetic resonance imaging (MRI).

***Corresponding author:** *Yasser. H. El-Sharkawy, Military Technical College, Department of Biomedical Engineering, MTC, Cairo, Egypt, E-mail: yhmelsharkawy@yahoo.com*

Received: March 17, 2016: **Accepted:** May 24, 2016: **Published:** May 27, 2016

Citation: El-Sharkawy YH (2016) Optical Properties of Non-Malignant and Malignant Breast Tissue Determined by Surface Displacement of Laser-Induced Photoacoustic Generation. Int J Opt Photonic Eng 1:002

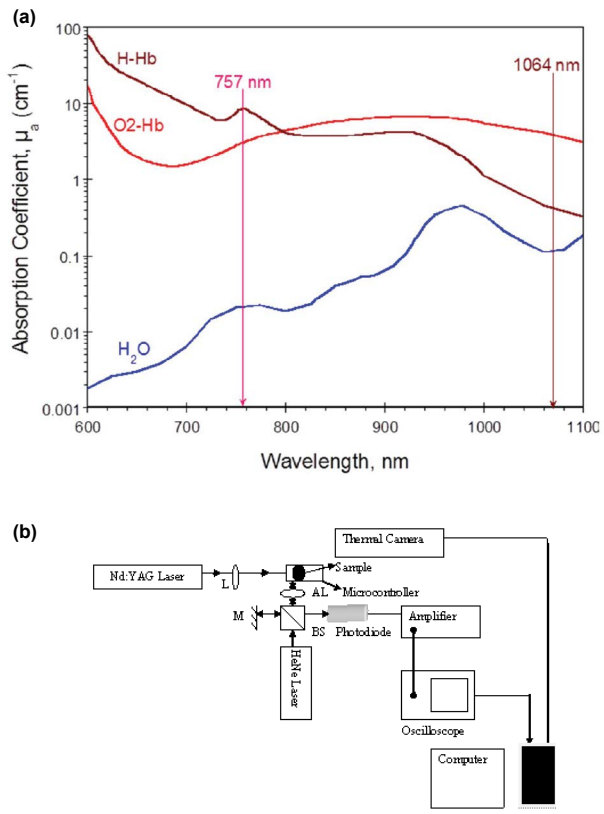

Figure 1: Laser photoacoustic and photothermal imaging (a) Optical absorption spectra of 3 major substances in tissue (Hb, HbO_2 and H_2O) that contribute to opto-acoustic image brightness, (b) Schematic diagram of the laser surface inter ferometric.

The technique of laser photoacoustic (PA) spectroscopy has been used in trace detection due to the high sensitivity it offers. In this method, a high-energy laser beam is used to irradiate the matter under study [18-20]. The beam produces a thermal expansion in the matter, thereby generating an acoustic wave. The characteristics of the wave are determined not only by the optical absorption coefficient of the matter, but also by such thermal physical parameters as thermal expansion, specific heat and sound velocity. In addition, the acoustic wave may also be affected by optical scattering which influences the distribution of light in the matter.

Laser-induced photoacoustic imaging used to characterize biological tissues [21]. In This technique Q-switched excimer laser at a wavelength 193nm and pulse duration 8ns interact thin polymer film (20 μm) placed on the sample surface producing high frequency acoustic waves at polymer layer (33 MHz) which propagate in the sample. A high frequency acoustic wave reflects back at tumor position mismatch. The disadvantage of the high resolution imaging system is the very low penetration depth in the tissue and small signal to noise ration.

Breast cancer, above a few millimeters in diameter, initiate very active angiogenesis, believed to be characteristic of all rapidly growing tumors. The increase of blood vessels does nevertheless fail to deliver adequate oxygen to the tumor and thus most tumors are hypoxic. Therefore the optical technique, with its unique ability to measure oxygenation state and blood volume content represents an excellent candidate for cancer diagnosis. The optical method, being a functional probe, offers a new dimension for tumor differentiation that promises to offer enhanced detection specificity, especially when combined with the sensitivity and high resolution of existing imaging methods.

In our paper a significant investigation of the dependence described photoacoustic signature on optical absorption. Since the photoacoustic response of breast tissue is dependent upon the optical and acoustic properties of the tissue, the mechanism by which thermo elastic waves are generated by the absorption of nanosecond Nd: YAG laser pulses which have the maximum penetration depth and highly absorbed by breast cancer tissue.

Laser illumination at the wavelength of 1064 nm provides contrast based mainly on the hypoxic blood of breast carcinomas, produces contrast dominated by the enhanced water content and normally oxygenated blood in benign fibro adenomas as shown in (Figure 1a). Detection of the resulting ultrasound signals with a inter ferometry laser probe preserves quantitative information about the tumor optical absorption. Investigation for breast cancer identification by classify the breast cancer samples to 3 groups first grad, second grad, and third grad samples, and analysis of photoacoustic response result to make pattern recognition are discussed.

Theoretical Investigation

The energy conversion from electromagnetic (light) energy to the acoustic wave occurs significantly faster than the stress relaxation or heat diffusion. Due to inertia of the sample, this process is physically an isochoric pressure rise / change. The ignition in an internal combustion engine serves as an illustrative analog on here to. When the gasoline-air mix is ignited, heat is brought into the system, and because of the piston's inertia, the temperature increase leads to an instantaneous pressure increase. Generally, stress and thermal confinement are provided. With only a few principles of mechanics of continua, the differential equation governing the acoustic propagation is derived. At first, the medium displacement u in dependence of pressure p and temperature T.

The photoacoustic wave generation and propagation in an in viscid medium is described by the general photoacoustic equation

$$\rho\frac{\partial^2 u}{\partial t^2}-E\nabla\frac{2u}{2(1+v)}-E\nabla\frac{(\nabla.u)}{2(1+v)(1-2v)}=-E\beta\nabla\left[\frac{T}{3(1-2v)}\right] \quad (1)$$

where u denotes the displacement vector, E is Young's modulus; v is Poisson's ratio, β is the thermal expansion coefficient and T is the laser-induced temperature increase above a uniform ambient level.

The general photoacoustic equation can be solved by numerical model that solves the thermo elastic wave equation (2) as a function of time and space in cylindrical has been carried out. Using finite element method, the displacement as a function of time and position has been determined. After the transient stress has passed, the sample attains quasi steady state equilibrium and will remain in this deformed state until thermal diffusion occurs. The equilibrium surface displacement u $(0,0,t > 1/\mu_{eff}\, C)$, in terms of laser fluency, equilibrium surface displacement on- axis u (r = 0, z = 0) is [1]

$$u\,(0,0,t > 1/\mu_{eff}\, C) = 2(1+v)\,\beta g(R)\Phi/3\rho\, Cv \quad (2)$$

where $1/\mu_{eff}\, C$ is the acoustic relaxation time, the function g(R) is a geometrical correction factor that describes the significance of aspect ratio $R = \varpi/D_{eff}$ and ϖ is the beam radius.

Experimental Investigation

Experiment

The developed photoacoustic system is shown in figure 1b. It is composed of a high pulse energy laser produced from Q- switched Nd: YAG laser at a wavelength 1064 nm and pulse duration 8ns, and optics arrangement for illumination control provides 8mm diameter spot on thin polymer film (20 μm) placed on the sample surface as shown in (Figure 1b).

The inter ferometric probe light from a CW He-Ne laser. A 50/50 beam splitter is used in a Michelson inter ferometer set-up. A 5 cm

lens focuses the light onto the sample through the polymer film. The sample motion modulates the frequency of the fringe pattern, and one can determine the direction and the speed of the sample surface. Due to the thermal diffusion the refractive index of thin polymer film has changed after thermal relaxation occur. The light is combined and directed towards photodiode. The photodiode signal is captured and digitized at a rate of 20 giga sample/sec by a digital oscilloscope and transferred to a computer for analysis.

Results and Discussion

First, we investigate the feasibility of using Photoacoustic techniques for identification of malignant in freshly excited breast tissue.

Within a reasonable range of tumor size, 10-30 mm^3, there is an increase of one degree Kelvin. Since the instrument that is used to measure the surface photoacoustic displacement and temperature are measured using inter ferometric probe light from a CW He-Ne laser and infrared camera that has an accuracy rate of ± 0.03°C, it is likely that the slight increase in temperature is significant and can be correctly identified for tumor detection.

Fresh tissue procured during breast conserving surgery was obtained directly from the Department of Pathology from patients who did not decline this use of their tissues. Tissues imaged by the optical imaging system are shown in figure 4. Specimen imaging did not affect procedure time in the operating room or the content and verification of the final pathology report. Tissues were imaged within 10 minutes of resection and returned to pathology for standard histological processing.

Figure 2a and figure 3a illustrate a digital photograph taken from the non-malignant and malignant breast samples of a 55-year-old patient affected by breast cancer, the affected tissue of size 2 cm^3. All samples of more than 12 biopsies (some of this irradiated sample are seen at end of this section in rainbow styles) were irradiated for 10 s at Q switching Nd: YAG laser at wavelength of 1064 nm show the following results.

Figure 2 and figure 3 shows the time dependent surfaced is placement for cancerous tumor breast tissue and normal breast tissue. Initial stress is proportional to the temperature distribution, and the initial displacements are zero. The surface expands in response to the stress distribution. A maximum in surface displacement occurs at 70 ns for cancerous tumor breast tissue and 116 ns for normal breast tissue following absorption of the 8ns pulse. This peak corresponds with the time needed for longitudinal acoustic waves from the beam edge to reach the center. The depth of the tumor can be determined by mapping to the acoustical axis z that is equal to acoustic speed multiplied by the time.

The initial rising slope of the photoacoustic response was determined by attenuation coefficient and longitudinal acoustic velocity of the tissue. As described above, acoustic velocity was found from the peak displacsssement, and then the effective penetration depth was used to fit the rising slope of the curve. The surface then falls to its quasi-steady state equilibrium value. As the Equilibrium displacement is varying with laser fluency, the ratio of the thermal expansion coefficient to heat capacity can be found from equation (2).

The photoacoustic surface displacement peak displacement is 1.7 (Arbiter units) and 2.56 (Arbiter units) for non-malignant and malignant breast tissue respectively, which matches the temperature distribution of the tissue photothermal image illustrated in figure 4. This means that the absorption coefficient of the tumor at 1064 nm is almost twice higher than the normal tissue.

The characteristics of the photothermal response such as the measured amplitude, rise time and decay time of the photothermal wave, depend on both optical properties and thermal properties of the tissue. By measuring the surface temperature under different conditions such as variations in tumor size, location, blood perfusion rate and heat transfer coefficient, we examined the temperature difference between two points on the breast to determine if the area of the tumor was significantly higher than an area farther away from the tumor. Representative images of thermal radiation from excited sample classification results due to changes on the temperature

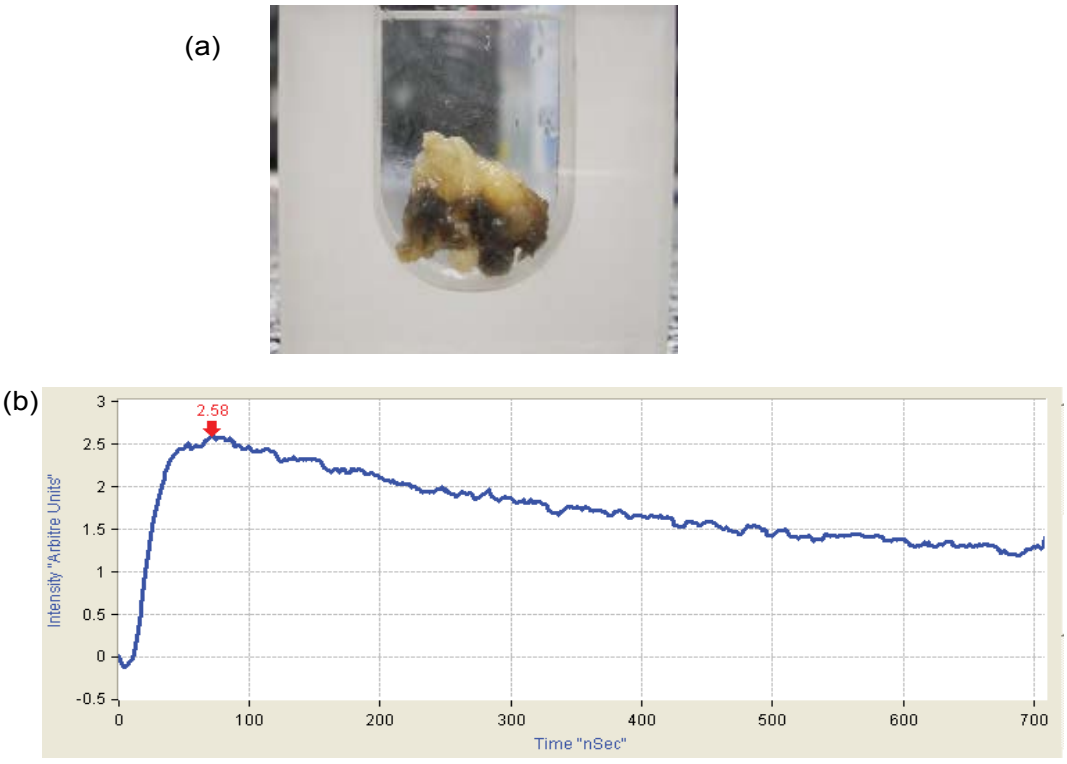

Figure 2: Breast cancer detection, (a) Illustrate a digital photograph taken from the breast samples of a 55-year-old patient affected by breast cancer, (b) Time induced Photoacoustic response of breast tumor.

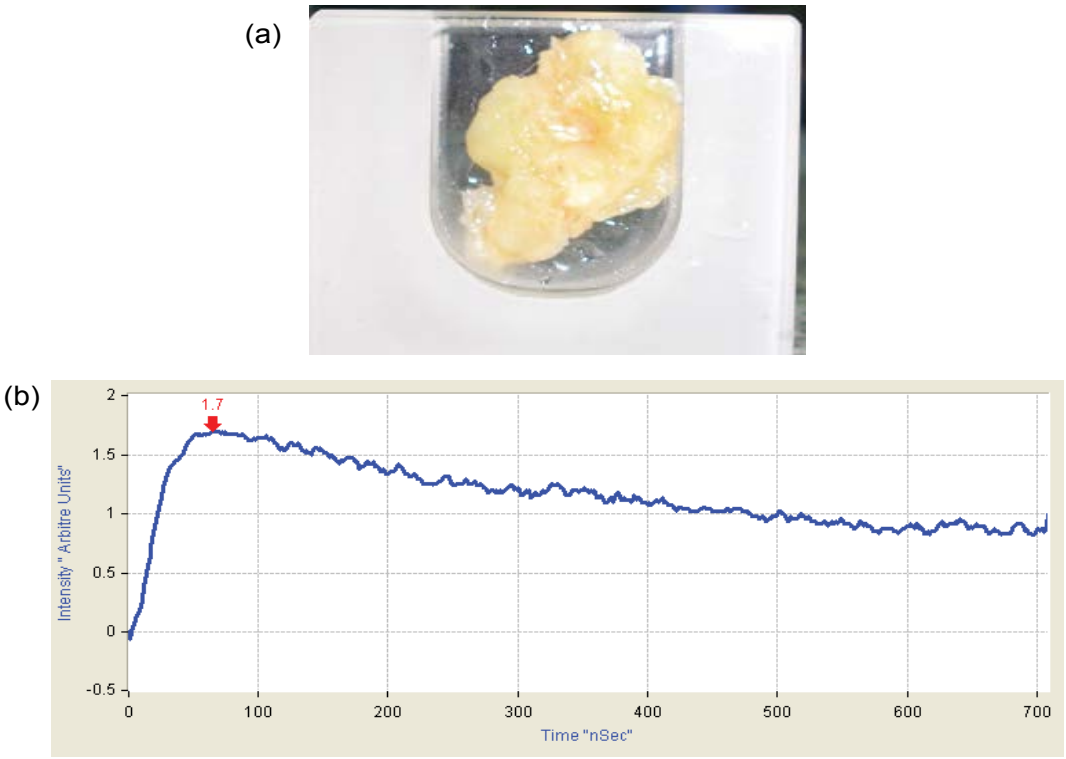

Figure 3: Breast cancer detection, (a) Illustrate a digital photograph taken from the breast samples of a 55-year-old patient affected by breast cancer, (b) Surface displacement and Photoacoustic signal of normal breast tissue measured by laser interferometer.

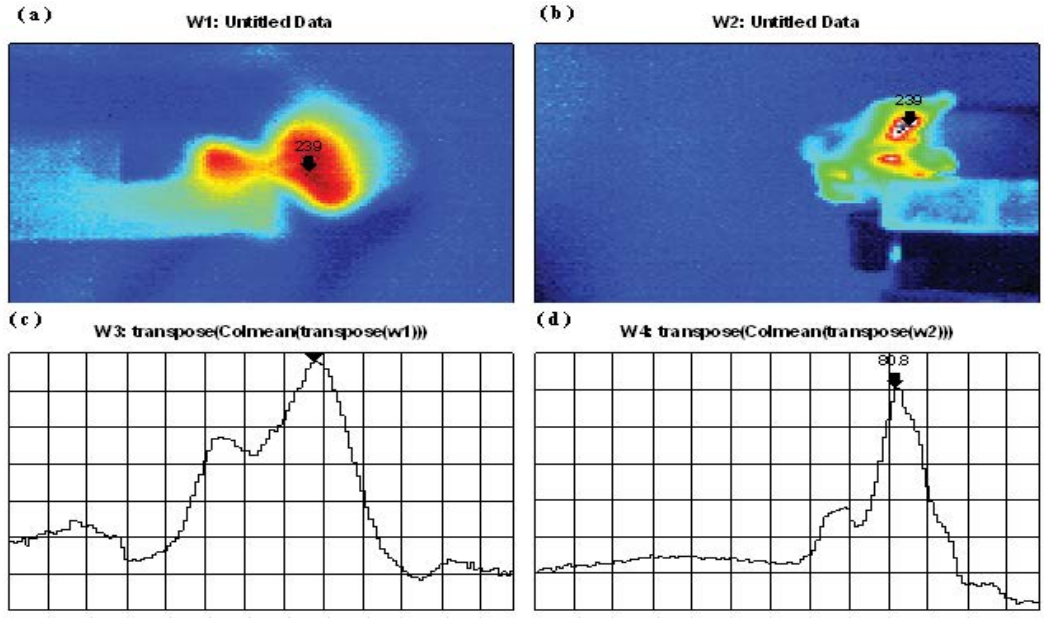

Figure 4: 2-D photo thermal images for Breast tumor sample captured by high sensitive thermal camera after sample excited by 1064 nm Q-switched Nd: YAG laser (a) Sample 1 for 55 years patient, (b) Sample 1 for 45 years patient, (c) photo thermal response of sample 1, (d) photo thermal response of sample 2.

gradient from non-malignant and malignant tissues at 1064 nm was monitored continuously by thermal camera of the surgical tissue for all diagnostic classes are shown in (Figure 4). Tumor position and malignant tissue can be classified according to high intensity of thermal radiation, which are calculated using the three-dimensional temperature distribution in the breast tissue after laser exposure

$$(T(r,z) \cong T_0\, e^{(-\mu_{eff} z)})$$

The intensity images of typical in vivo two affected breast samples in the first and second windows of figure 4a and figure 4b show significant deviation from non-malignant and malignant tissue. The photothermal radiation intensity increased linearly with most affected tissue and then tumors position can be discriminated as shown in (Figure 6).

In other words, for malignant areas, the absorption coefficient is higher than that of the non-malignant (normal) parts, which confirmed with the Photoacoustic response measured for the same samples. This is the reason for the direct proportionality between

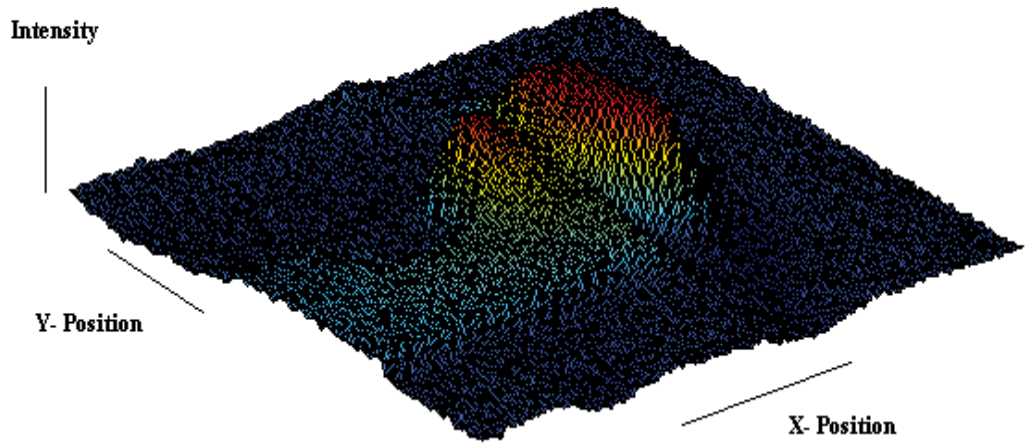

Figure 5: 3-D photo thermal image plot for breast tumor tissue.

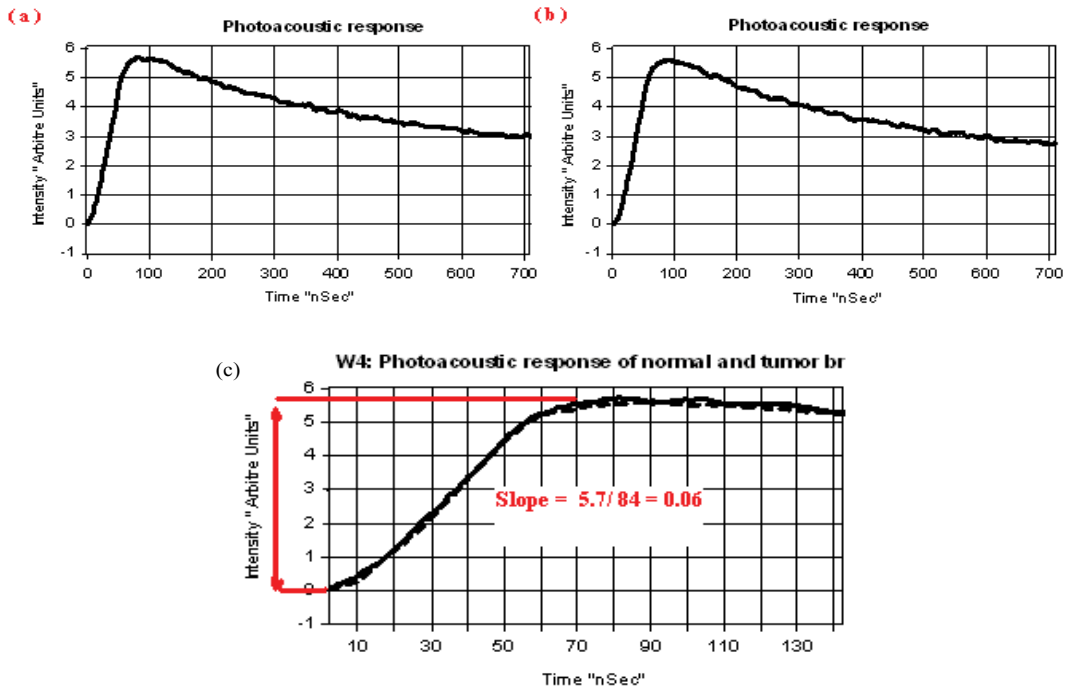

Figure 6: Photoacoustic responses of (a) normal (non-malignant) tissue, solid line, (b) tumor (malignant) tissue, (c) attenuation coefficients calculated from Photoacoustic response. Normal (non-malignant) solid line and tumor (malignant) tissue dashed line.

the amplitude of the peak at the tumor position with the level of the cancer grads as shown in 3 D image plotting illustrated in (Figure 5).

Figure 4c and figure 4d show the measured time course of the changes in temperature following the absorption of 8ns laser pulse in breast tumor and normal tissue sample. The high intensity photothermal wave was induced from diffusion of heat from the laser-heated volume to the surrounding cooler areas. This was a much slower process and was observed in a time extending to as much 10.

Breast cancer, above a few millimeters in diameter, initiate very active angiogenesis, believed to be characteristic of all rapidly growing tumors. The increase of blood vessels does nevertheless fail to deliver adequate oxygen to the tumor and thus most tumors are hypoxic. Therefore the photoacoustic technique, with its unique ability to measure physical, optical, and acoustical properties of tumors state and blood volume content represents an excellent candidate for cancer diagnosis. The optical method, being a functional probe, offers a new dimension for tumor yield highly sensitive early cancer detection modality. It is envisaged that molecular-level probing will lower the limits of early cancer detection since detection can occur before anatomic changes, usually detected by common radiologic techniques become apparent.

Calculation of optical properties

The results of this study show that in the presence of a tumor in the breast, there is a significant difference, 3-5°C for a respective diameter range of 10 mm-30 mm, in the surface temperature of the breast above its location when compared to normal tissue. Analysis of photothermal imaging illustrated in figure 4 can therefore be used to indicate the possible presence of a tumor within the breast, but it cannot be used as an accurate predictor because variations in the heat transfer coefficient, blood perfusion rate and tumor location that can be significant enough to throw off the temperature analysis. In actual practice, results may also not be so clear with variations in breast tissue like density and other normal inconsistencies, producing unexpected results. Since a photothermal response is not efficient enough by itself, a photoacoustic response analysis was performed on the model that showed a 10 mm diameter tumor at location. These structures are found embedded beneath epithelial layers and required selecting probing laser beam capable to penetrate the tissue

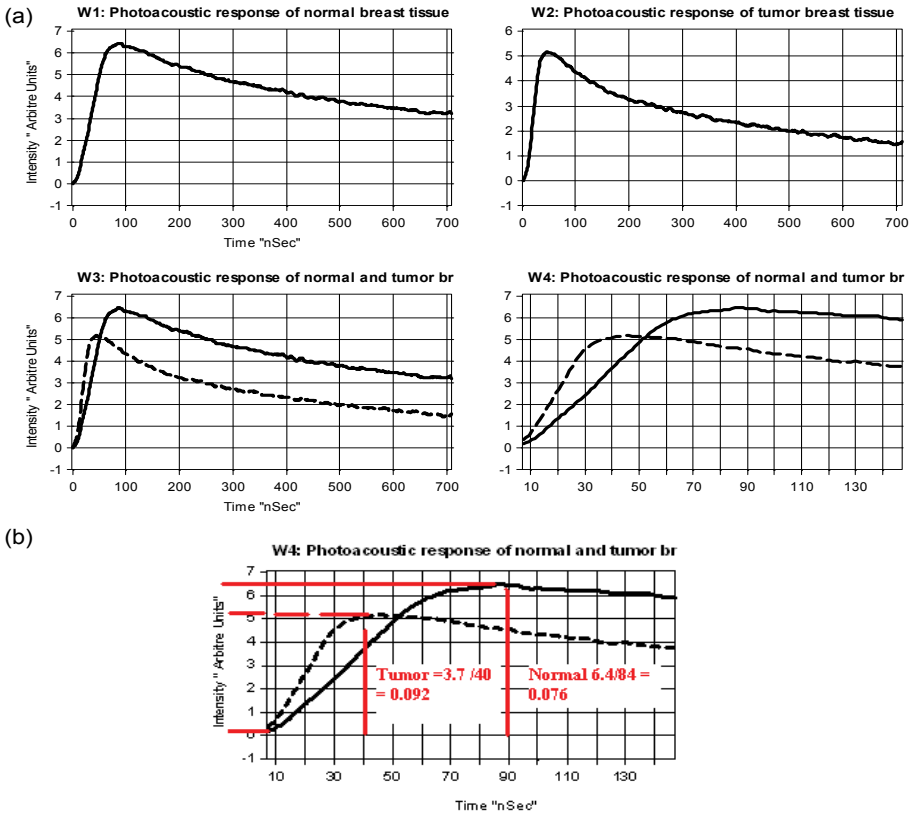

Figure 7: Photoacoustic responses of (a) normal (non-malignant) solid line and tumor (malignant) tissue dashed line, (b) attenuation coefficients calculated from Photoacoustic response.

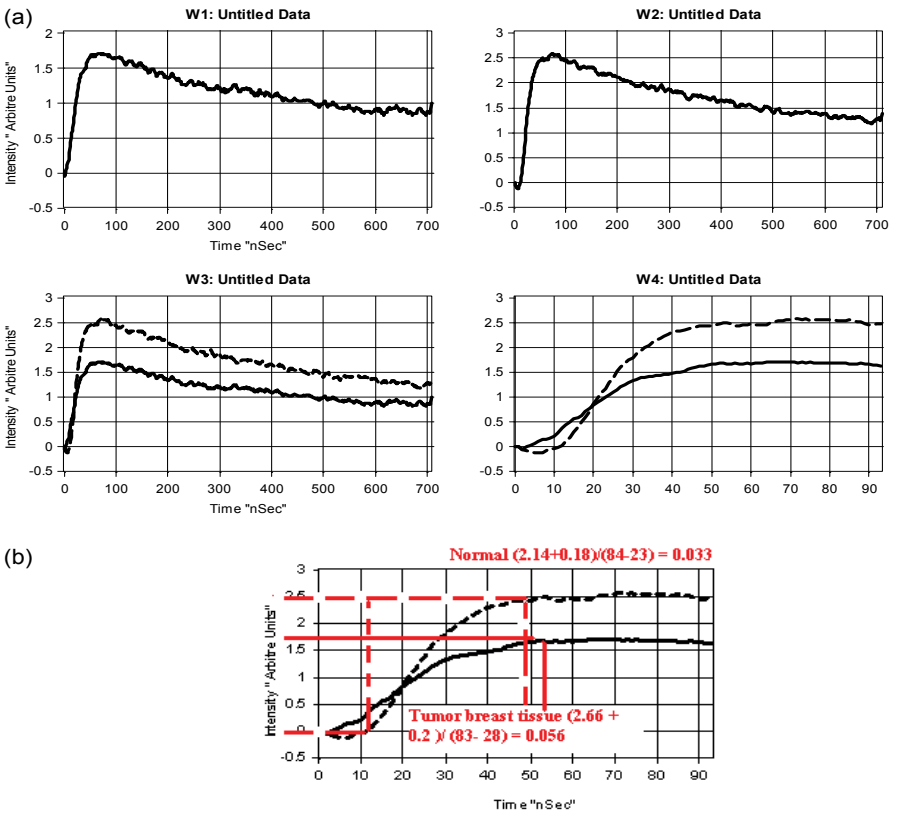

Figure 8: Photoacoustic responses of (a) normal (non-malignant) solid line and tumor (malignant) tissue dashed line, (b) attenuation coefficients calculated from Photoacoustic response.

Table 1: Attenuation coefficient calculated by photoacoustic response, thermal conductivity, and laser heat production.

Tissue Layer	Attenuation coefficient calculated by photoacoustic response	Thermal conductivity k (W/m°C)	Laser heat production qm (W/m³)
Tumor (20 mm)	0.092	0.61	5810
Tumor (30 mm)	0.06	0.48	5790
Tumor (40 mm)	0.056	0.47	5785

and highly absorbed by malignant area. Figures 6, figure 7, and figure 8 depict the photoacoustic response of normal and malignant breast tissue, for three different patient statuses. In order to find the best way of detecting and locating lesions and tumors, by determine the tissue attenuation coefficient using Photoacoustic response.

The tumors of the first sample had an average size of 22 mm^3 in the start of irradiation. Photoacoustic response and Thermal images, taken at various time points during the heating, showed that the tissue heated up very fast and reached an average temperature of 39°C.

By contrast, the tumors reached temperatures of more than 40°C after 5 s, while the laser spot size was much greater than the tumor (30 mm as compared with a tumor size of less for comparison, we examined the NIR photothermal heating capabilities of 1064 nm. Figure 6a and figure 6b illustrate the Photoacoustic response of the normal and tumor breast tissue of the patient, respectively. The calculated attenuation coefficients of the two samples are 0.06 cm^{-1} as shown in (Figure 6c). This value is reasonable since the patient biological exam is normal with high degree of accuracy and matching with the physician report.

Figure 7 w1 and w2 illustrate the Photoacoustic response of the normal and tumor breast tissue of the patient, respectively. The calculated attenuation coefficients of the normal and tumor breast tissue are 0.076 and 0.092 cm^{-1}, respectively as shown in figure 7b. A histological exam following Photoacoustic technique has shown that this tumor is a papillary cancer, whose size has been determined, after surgery, to be 1.6 cm.

A sensitivity analysis was conducted to determine the effects that variations in tissue parameters had on the outcome of the photoacoustic and photothermal responses. Examining for such differences allows checking the accuracy of the results. Our focus was the effects that the size of the tumor, the location, the blood perfusion rate of the tumor and the heat transfer coefficient has on the surface temperature of the breast (Figure s1 and Figure s2). Normal values used for analysis and variations are shown in (Table 1).

Figure 8 w1 and w2 illustrate the Photoacoustic response of the normal and tumor breast tissue of the patient, respectively. The calculated attenuation coefficients of the normal and tumor breast tissue are 0.033 and 0.056 cm^{-1}, respectively as shown in figure 8b. A histological exam following Photoacoustic technique has shown that this tumor is a cancer, whose size has been determined, after surgery, to be 2 cm. The measured equilibrium displacement can be utilized as described above to determine the Grüneisen coefficient Γ, of the breast sample. For comparison the higher values of Grüneisen coefficient denote that the tumor be more solid than the normal breast tissue.

Conclusion

Optical properties derived by photoacoustic techniques can be used to constructed high resolution functional maps and provide law cost diagnostic tool. The difference in the slopes of this variation of photoacoustic response generated the contrast to differentiate and identify the malignant and non-malignant in the breast. These initial investigations using photoacoustic and photothermal imaging of breast suggests the possibility to simultaneously image and identification the breast cancer.

References

1. A Dhahir R K, Dyer P E, Zhu Z (1990) Photoacoustic studies and selective ablation of vascular tissue using a pulsed dye laser. Appl Phys B 51: 81-85.
2. (1990) National Institutes of Health Consensus Development Conference Statement: Treatment of Early Breast Cancer 18-21.
3. (1992) American Cancer Society: Cancer Facts & Figures-1992. Atlanda, American Cancer Society.
4. O'Maley M, Fletcher S, Morrison B (1990) "Does Screening for Breast Cancer Save Lives? Effectiveness of Treatment After Breast Cancer Detection Following Screening by Clinical Breast Examination, Mammography and Breast Self-examination", New York, NY: Springer-Verlag New York Inc.
5. Andersson I, Aspegren K, Janzon L, Landberg T, Lindholm K, et al. (1988) Mammographic screening and mortality from breast cancer: the Malmö mammographic screening trial. BMJ 297: 943-948.
6. Roberts MM, Alexander FE, Anderson TJ, Chetty U, Donnan PT, et al. (1990) Edinburgh trial of screening for breast cancer: mortality at seven years. Lancet 335: 241-246.
7. Frisell J, Eklund G, Hellstrom L, Lidbrink E, Rutqvist LE, et al. (1991) Randomized study of mammography screening: preliminary report on mortality in the Stockholm trial. Breast Cancer Res Treat 18: 49-56.
8. Shapiro S, Venet W, Strax P, Venet L, Roeser R (1982) Ten- to fourteen-year effect of screening on breast cancer mortality. J Natl Cancer Inst 69: 349-355.
9. Tabar L, Fagerberg CJ, Gad A, Baldetorp L, Holmberg LH, et al. (1985) Reduction in mortality from breast cancer after mass screening with mammography. Randomized trial from the Breast Cancer Screening Working Group of the Swedish National Board of Health and Welfare. Lancet 1: 829-832.
10. Verbeek AL, Hendriks JH, Holland R, Mravunac M, Sturmans F, et al. (1984) Reduction of breast cancer mortality through mass screening with modern mammography. First results of the Nijmegen project, 1975-1981. Lancet 1: 1222-1224.
11. Adair F, Berg J, Joubert L, Robbins GF (1974) Long-term followup of breast cancer patients: the 30-year report. Cancer 33: 1145-1150.
12. Carter CL, Allen C, Henson DE (1989) Relation of tumor size, lymph node status, and survival in 24,740 breast cancer cases. Cancer 63: 181-187.
13. Kerlikowske K, Grady D, Barclay J, Sickles EA, Ernster V (1996) Likelihood ratios for modern screening mammography. Risk of breast cancer based on age and mammographic interpretation. JAMA 276: 39-43.
14. Kerlikowske K, Grady D, Barclay J, Sickles EA, Eaton A, et al. (1993)Positive predictive value of screening mammography by age and family history of breast cancer. JAMA 270: 2444-2450.
15. Sickles EA (1991) Periodic mammographic follow-up of probably benign lesions: results in 3,184 consecutive cases. Radiology 179: 463-468.
16. Cyrlak D (1988) Induced costs of low-cost screening mammography. Radiology 168: 661-663.
17. Andersson-Engels S, Johansson J, Stenram U, Svanberg K, Svanberg S (1990) Malignant tumor and atherosclerotic plaque diagnosis using laser induced fluorescence. IEEE Journal of Quantum Electron 26: 2207-2216.
18. Baraga JJ, Feld MS, Rava RP (1992) In situ optical histochemistry of human artery using near infrared Fourier transform Raman spectroscopy. Proc Natl Acad Sci USA 89: 3472-3477.
19. Beard PC, Mills TN (1995) Evaluation of an optical fibre probe for in vivo measurement of the photoacoustic response of tissues. Proc SPIE 2388: 446-457.
20. Dark ML, Perelman LT, Itzkan I, Schaffer JL, Field MS (1999) physical properties of hydrated tissue determined by surface interferometry of laser-induced thermo elastic deformation. Phys Med Biol 45: 529-539.
21. Yasser H El-Sharkawy, Yehia Badr (2005) Laser-induced photoacoustic imaging for characterizing biological tissues. Proc SPIE 5689: 165.

Citation: El-Sharkawy YH (2016) Optical Properties of Non-Malignant and Malignant Breast Tissue Determined by Surface Displacement of Laser-Induced Photoacoustic Generation. Int J Opt Photonic Eng 1:002

Figure S1: Different breast samples classified by physicians Photothermal imaging results of the samples.

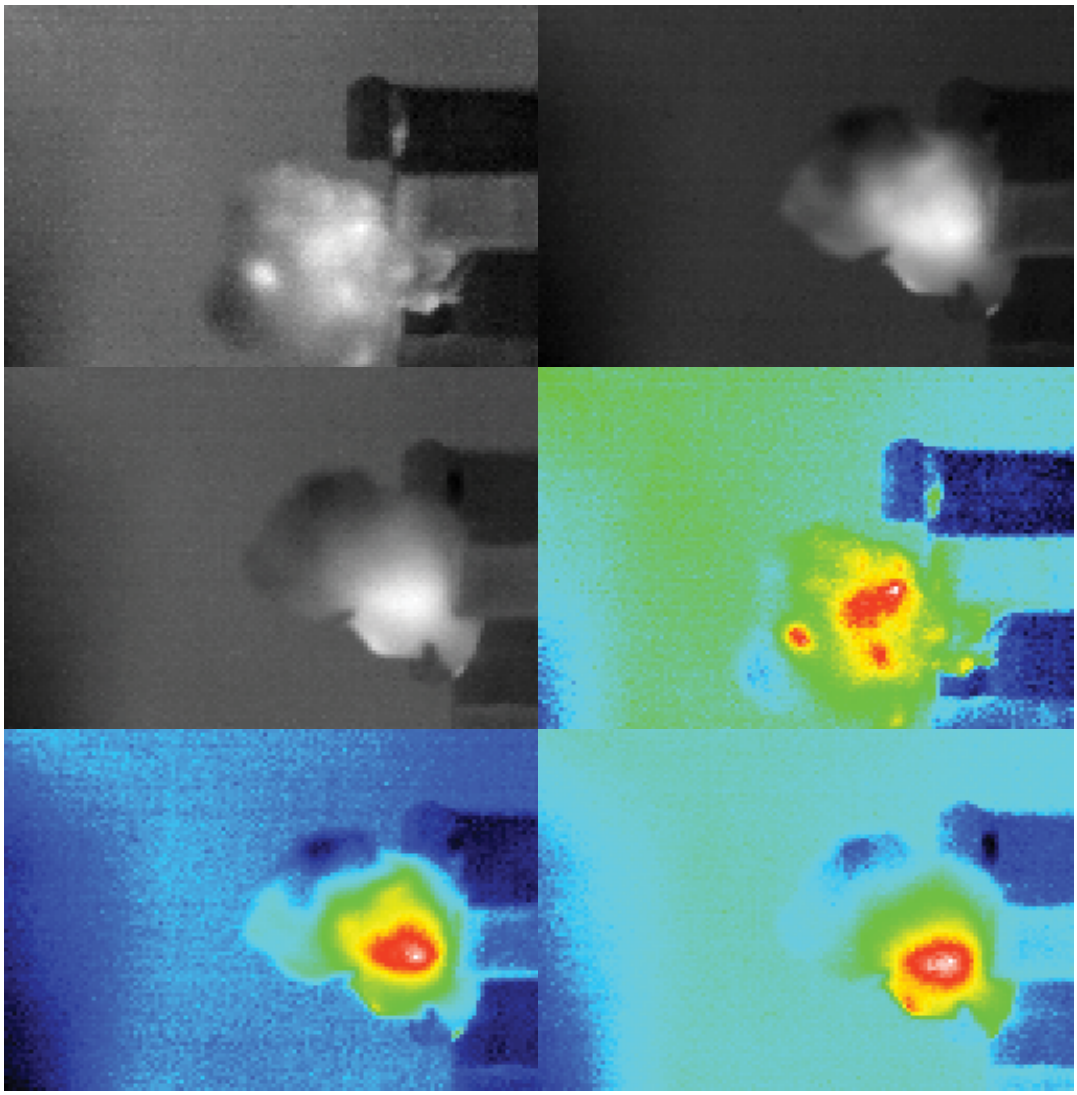

Figure S2: Shows the relationship between the tumor location and the change in surface temperature that goes with each tumor location. Different locations (see Appendix C for details) change the surface temperature appreciably, from 306.14 K at location 1 to 302.71 K at location 5. Comparing Figure 2 to Figure 1, tumor location is a much more sensitive factor than tumor size. Our analysis will be based on the first two locations for optimum results.

Citation: El-Sharkawy YH (2016) Optical Properties of Non-Malignant and Malignant Breast Tissue Determined by Surface Displacement of Laser-Induced Photoacoustic Generation. Int J Opt Photonic Eng 1:002